Doc Ophthalmol (2015) 130:149–156
DOI 10.1007/s10633-014-9478-2

ORIGINAL RESEARCH ARTICLE

Molecular, anatomical and functional changes in the retinal ganglion cells after optic nerve crush in mice

Masayoshi Yukita · Shigeki Machida · Koji M. Nishiguchi · Satoru Tsuda · Yu Yokoyama · Masayuki Yasuda · Kazuichi Maruyama · Toru Nakazawa

Received: 21 October 2014 / Accepted: 30 December 2014 / Published online: 6 January 2015

Abstract
Purpose Optic nerve crush (ONC) and subsequent axonal damage can be used in rodents to study the mechanism of retinal ganglion cell (RGC) degeneration. Here, we examined electroretinograms (ERGs) in post-ONC mice to investigate changes in the positive scotopic threshold response (pSTR). We then compared these changes with molecular and morphological changes to identify early objective biomarkers of RGC dysfunction.
Methods Fifty 12-week-old C57BL/6 mice were included. ONC was used to induce axonal injury in the right eye of each animal, with the left eye used as a control. The expression of the RGC markers *Brn3a* and *Brn3b* was measured on days 1, 2, 3, 5 and 7 after ONC with quantitative real-time PCR. ERGs were recorded under dark adaptation with the stimulus intensity increasing from −6.2 to 0.43 log cd-s/m^2 on days 1, 2, 3, 5, 7 and 10 after ONC. The pSTR, a- and b-wave amplitudes were measured. Inner retinal thickness around the optic nerve head was measured with spectral-domain optical coherence tomography on days 0, 2, 5, 7 and 10 after ONC.
Results The expression of *Brn3a* and *Brn3b* began to significantly decrease on day 1 and day 2, respectively ($P < 0.01$). The amplitude of the pSTR underwent rapid, significant deterioration on day 3, after which it fell gradually ($P < 0.01$), while the a- and b-wave amplitudes remained unchanged throughout the experiment. Inner retinal thickness gradually decreased, with the most significant reduction on day 10 ($P < 0.01$).
Conclusions Decrease in pSTR likely reflected the early loss of RGC function after ONC and that declining expression of RGC-specific genes preceded anatomical and functional changes in the RGCs.

M. Yukita · S. Tsuda · Y. Yokoyama · M. Yasuda · K. Maruyama · T. Nakazawa (✉)
Department of Ophthalmology, Tohoku University Graduate School of Medicine, 1-1 Seiryo, Aoba, Sendai, Miyagi 980-8574, Japan
e-mail: ntoru@oph.med.tohoku.ac.jp

S. Machida
Department of Ophthalmology, Dokkyo Medical University Koshigaya Hospital, Saitama, Japan

S. Machida
Department of Ophthalmology, Iwate Medical University School of Medicine, Morioka, Japan

K. M. Nishiguchi · T. Nakazawa
Department of Advanced Ophthalmic Medicine, Tohoku University Graduate School of Medicine, Sendai, Miyagi, Japan

T. Nakazawa
Department of Retinal Disease Control, Tohoku University Graduate School of Medicine, Sendai, Miyagi, Japan

Keywords Axonal injury · Glaucoma · Retinal ganglion cell · Electroretinogram · Scotopic threshold response

Introduction

Currently available treatments for glaucoma mostly depend on lowering intraocular pressure (IOP) [1]. However, even after the successful reduction in IOP, visual dysfunction continues to progress in many glaucoma patients [2], likely due to the influence of IOP-independent contributing factors [1–3] such as axonal injury [2]. Thus, new therapies targeting these factors have been the subject of recent research and development.

Animal models are one of the most useful tools for understanding the pathogenesis of disease and developing new treatments. Research on retinal ganglion cell (RGC) degeneration commonly uses optic nerve crush (ONC) in rodents as an animal model [4, 5]. However, despite numerous previous studies of ONC-induced morphological and molecular changes in the RGCs [6, 7], early sequential change in RGC function, especially its relationship with alterations in gene expression, remains poorly understood.

The photopic negative response (PhNR) [8] of the photopic electroretinogram (ERG) has emerged as a new functional measure of the RGCs in clinical practice [9–14]. However, studies have suggested that, in rodents, the PhNR originates from amacrine cells [15] and is thus unaffected by ONC [15, 16]. A useful alternative may be the scotopic threshold response (STR) of the scotopic ERG, which is elicited by very dim stimuli and is driven by the inner retina, including the RGCs [17, 18]. The STR consists of negative and positive components, defined as the positive STR (pSTR) and negative STR (nSTR), respectively [16]. In particular, the pSTR has been suggested to reflect RGC function in rodents [16, 19, 20]. However, it has not been determined at what time point after ONC alterations begin to occur in the pSTR caused by the functional loss of RGCs.

The aim of this study was therefore to determine whether the pSTR could serve as an early biomarker of RGC dysfunction after ONC in mice. We thus set out to compare changes in the pSTR with molecular and morphological changes in the RGCs after ONC.

Methods

Animals

Fifty C57BL/6 mice (male, 12-week-old; SLC, Hamamatsu, Japan) were used in this study. All animals were handled in accordance with the guidelines of the ARVO Statement for the Use of Animals in Ophthalmic and Vision Research and the guidelines from the Declaration of Helsinki. All experimental procedures described were approved by the Ethics Committee for Animal Experiments of Tohoku University Graduate School of Medicine.

During the surgical procedures, recording of the ERGs and spectral-domain optical coherence tomography (SD-OCT) imaging, the mice were anesthetized with ketamine (100 mg/kg) and xylazine (9 mg/kg). In the ONC procedure, the optic nerve was exposed, crushed 1.0 mm posterior to the globe with fine forceps for 5 s and released [4]. This procedure was performed by a single surgeon in order to reduce variations in the severity of the ONC-induced damage. The contralateral eye was left untouched and served as a control.

Quantitative real-time PCR

Total RNA (200 ng per sample) extracted from the retina was first reverse transcribed into cDNA using SuperScript III (Invitrogen Life Technologies, Carlsbad, CA, USA). Quantitative real-time PCR (RT-PCR) was then performed in duplicate with a 7500 Fast RT-PCR System (Applied Biosystems, Foster City, CA, USA) as previously described [21]. To determine relative gene expression, we analyzed the RT-PCR data with the comparative Ct method ($2^{-\Delta\Delta CT}$), normalized to an

Table 1 List of Taqman probes used in this study

Gene symbol	Assay ID
Pou4f1	Mm02343791_m1
Pou4f2	Mm00454754_s1

endogenous control (*Gapdh*). The Taqman probes used for these reactions are listed in Table 1.

Recording the ERG

The mice were dark-adapted overnight and were prepared for the ERG recording under dim red light. Each animal underwent additional dark adaptation for approximately 30 min before starting the ERG recording. The mice were anesthetized with an intraperitoneal injection of a mixture of ketamine (100 mg/kg) and xylazine (10 mg/kg).

The pupils were maximally dilated with topical 0.5 % tropicamide and 0.5 % phenylephrine HCL, and the corneas were anesthetized with topical 0.4 % oxybuprocaine hydrochloride. A contact lens electrode embedded with gold wire was placed on the cornea as an active electrode (Mayo, Nagoya, Japan), and a chloride silver plate was placed in the mouth as a reference electrode. A grounded aluminum sheet placed under the animal served as the ground electrode. Body temperature was kept at 37 °C with a heating pad.

The ERGs were recorded from both eyes simultaneously using a Ganzfeld bowl that had originally been assembled at the Kellogg Eye Center (Ann Arbor, MI, USA). Responses were amplified 10,000 times and band-pass filtered from 0.3 to 500 Hz (PuREC PC-100, Mayo, Inazawa, Japan). Brief white stimuli were produced by a xenon arc lamp that was mounted on the top of the Ganzfeld bowl and controlled by a photic stimulator (PS33-PLUS, Grass Instruments, Quincy, MA, USA). The ERG was recorded under dark adaptation with increasing stimulus intensity from −6.2 to 0.43 log cd-s/m^2 in 0.40-, 0.23- or 0.37-log-unit steps. The flash duration was 10 μs. The response to approximately 20–30 flashes was recorded at each stimulus intensity, with an inter-stimulus interval of 3 s, and then averaged to determine the final value of the STR [16, 22, 23]. The pSTR and nSTR amplitudes were measured from the baseline to the peak of the first positive wave and from the baseline to the negative trough after the positive wave, respectively (Fig. 2a). In higher stimulus ranges, 2–3 responses were averaged with an inter-stimulus interval of 10–60 s, depending on the stimulus intensity. The a-wave amplitude was measured from the baseline to the trough of the first negative response and the b-wave amplitude from the first trough to the peak of the following positive wave.

SD-OCT imaging

After pupil dilation, hydroxymethylcellulose (Goniosol, 2.5 %; Alkon, Buffalo Grove, IL, USA) was applied to the cornea during the recording. Retinal images were then acquired by scanning circumferentially around the optic nerve head with spectral-domain optical coherence tomography (SD-OCT) (RS-3000 Advance, Nidek). The distance between the internal limiting membrane and inner plexiform layer was measured to determine inner retinal thickness.

Statistical analysis

A one-way repeated-measures ANOVA with a post hoc Bonferroni test was used to assess the post-ONC quantitative RT-PCR data. A two-way repeated-measures ANOVA with a post hoc Bonferroni test was used to compare the OCT data in the control and ONC eyes. A paired Student *t* test was performed to compare the STR amplitude in the control and ONC eyes. Average values are shown as the mean with standard error. Differences were considered significant at $P < 0.05$.

Results

Reduced RGC-specific gene expression after ONC

Functional and morphological changes in the RGCs likely accompany changes in RGC-specific gene expression. We therefore used RT-PCR to determine the time when generalized changes in gene expression took place in the RGCs following ONC. This was done by studying the temporal expression profile of two representative RGC-specific genes: *Brn3a* and *Brn3b,* which have been shown to represent defferent RGC types (Fig. 1). [24, 25] *Brn3a* showed the earliest decrease in expression, on day 1 (40.9 ± 13.4 % reduction, Bonferroni test, $P < 0.01$). This was followed by a decrease in *Brn3b* (65.9 ± 8.9 % reduction, Bonferroni test, $P < 0.01$) on day 2.

Intensity–response function after ONC

Figure 2 shows representative intensity–response series of the scotopic ERG for the control (black line) and ONC (red line) eyes on days 1 and 10. On day 1,

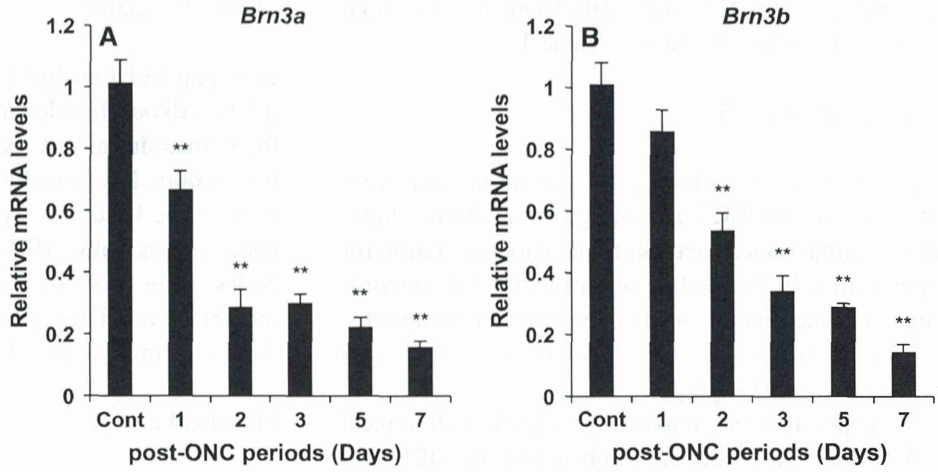

Fig. 1 The retinal mRNA levels of *Brn3a* (**a**) and *Brn3b* (**b**) were measured on days 1, 2, 3, 5, and 7 after ONC ($n = 6$ at each time point). There was a significant reduction in gene expression on day 1 for *Brn3a* and on day 2 for *Brn3b*. *ONC* optic nerve crush, *error bars* standard error, $^{**}P < 0.005$

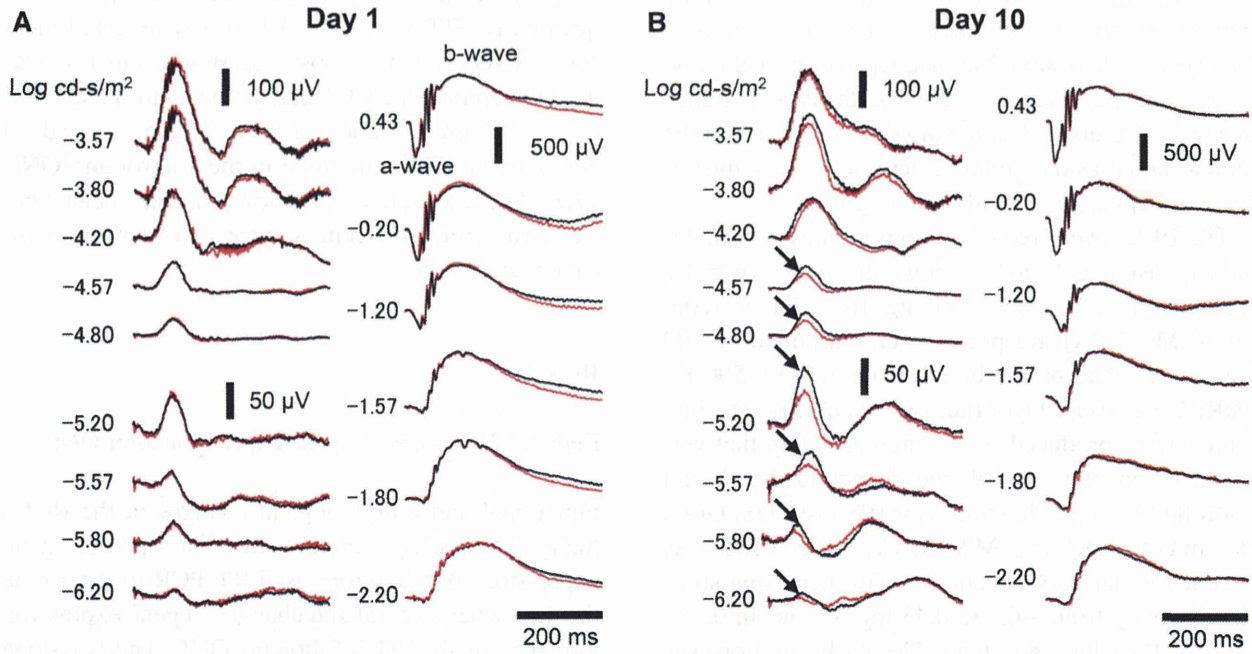

Fig. 2 Representative intensity–response ERG series recorded from control (*black lines*) and ONC (*red lines*) eyes on days 1 (**a**) and 10 (**b**) after ONC. The pSTR to low-intensity stimuli in the ONC eyes deteriorated on day 10 (indicated by the *arrows* in **b**). *ERG* electroretinogram, *ONC* optic nerve crush, *pSTR* positive scotopic threshold response

the waveforms completely overlapped over the entire stimulus range. On day 10, the pSTR in the lower stimulus range deteriorated in the ONC eyes relative to the control eyes (indicated by the arrows in Fig. 2b). The a- and b-waves of the control and ONC eyes elicited by stimuli of higher intensities completely overlapped. As there was no significant difference in the nSTR amplitude of the treated and untreated eyes at any stimulus intensity, we excluded nSTR results from our analysis.

The amplitude of the positive waves, including the pSTR and b-waves, was plotted against stimulus intensity to determine the intensity–response function on days 1, 2, 3, 5, 7 and 10 after ONC for the control (black symbols) and ONC (red symbols) eyes (Fig. 3a–f). The a-wave amplitude is also shown in the lower right of each figure. The intensity–response curves of the control and ONC eyes overlapped until day 2. In the lower stimulus range, the curve of the ONC eyes shifted downward and separated from the

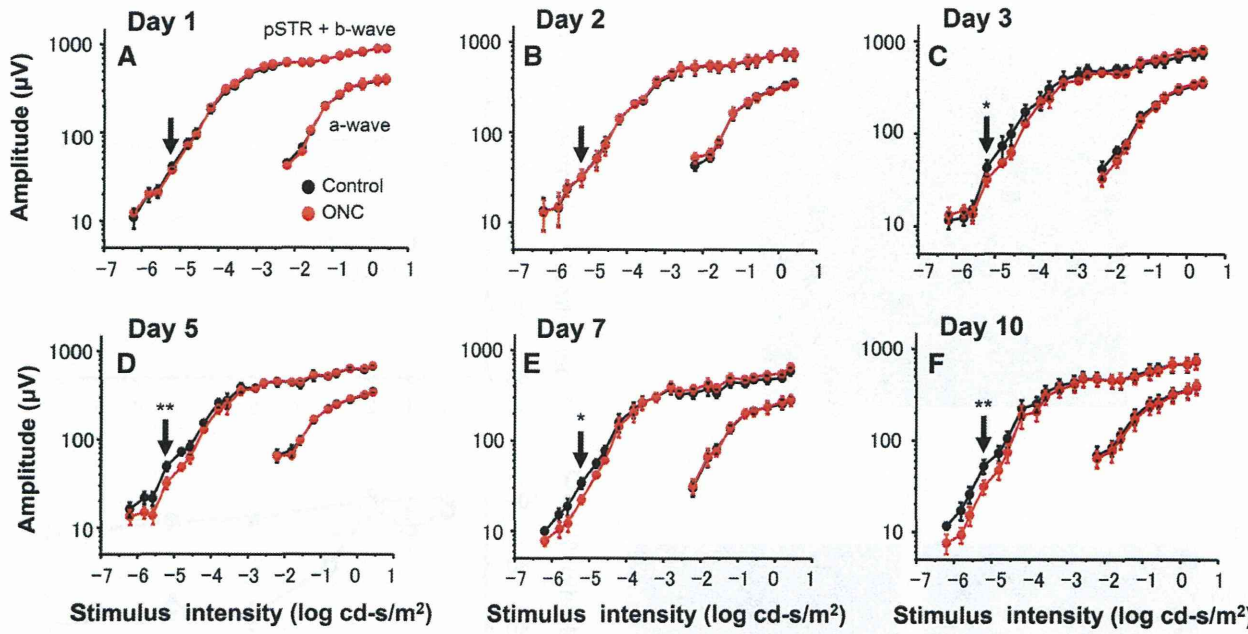

Fig. 3 Intensity–response functions for the pSTR + b-wave and a-waves recorded from control ($n = 5$, *black symbols*) and ONC ($n = 5$, *red symbols*) eyes on days 1 (**a**), 2 (**b**), 3 (**c**), 5 (**d**), 7 (**e**) and 10 (**f**) after ONC. The arrows in each figure indicate the pSTR amplitude elicited by a stimulus intensity of −5.2 log cd-s/m^2. *pSTR* positive scotopic threshold response, *ONC* optic nerve crush, *error bars* standard error, $*P < 0.01$, $**P < 0.005$

curve of the control eyes on day 3. On day 10, the maximum difference between the control and ONC eyes was seen, at the stimulus intensity of 5.2 log cd-s/m^2 (Fig. 3f). Therefore, subsequent analyses used the pSTR amplitude elicited at an intensity of −5.2 log cd-s/m^2 to compare the control and ONC eyes (indicated by the arrows in Fig. 3). Significant differences were seen in the pSTR amplitude between the control and ONC eyes after day 3 (paired *t* test, $P < 0.01$ for days 3 and 7; $P < 0.005$ for days 5 and 10).

Inner retinal thickness after ONC, measured with in vivo OCT imaging

Finally, we measured the thickness of the inner retina around the optic nerve head, as a morphological indicator of the status of the RGCs on days 1, 2, 3, 5, 7 and 10 after ONC (Fig. 4b). Figure 4b shows a representative OCT image, obtained on day 10, in which the selective loss of the inner retina is visible. After day 5, the inner retinal thickness gradually and progressively declined, with the most significant difference between the control and ONC eyes being seen on day 10 (Fig. 4c, Bonferroni test, $P < 0.01$).

Correlation between pSTR and inner retinal thickness

The pSTR amplitude and inner retinal thickness of the ONC eyes were normalized to those of the contralateral control eyes, expressed as a percentage and plotted as a function of the post-ONC period (Fig. 4d). A rapid loss in pSTR amplitude was seen on day 3, followed by a gradual loss over time, concurrent with the gradual loss of inner retinal thickness.

Discussion

In this study, we found that changes in the pSTR could be used to detect dysfunction of the RGCs as early as day 3 after ONC and that changes occurred in the pSTR earlier than in the OCT-measured morphology of the retina, which did not occur until day 10. Moreover, we previously used retrograde Fluorogold labeling of the RGCs to show that RGC loss began 5 days after ONC, suggesting that the alterations in the pSTR observed here occurred before even microscopic loss of the RGCs [4]. We have also previously found that in

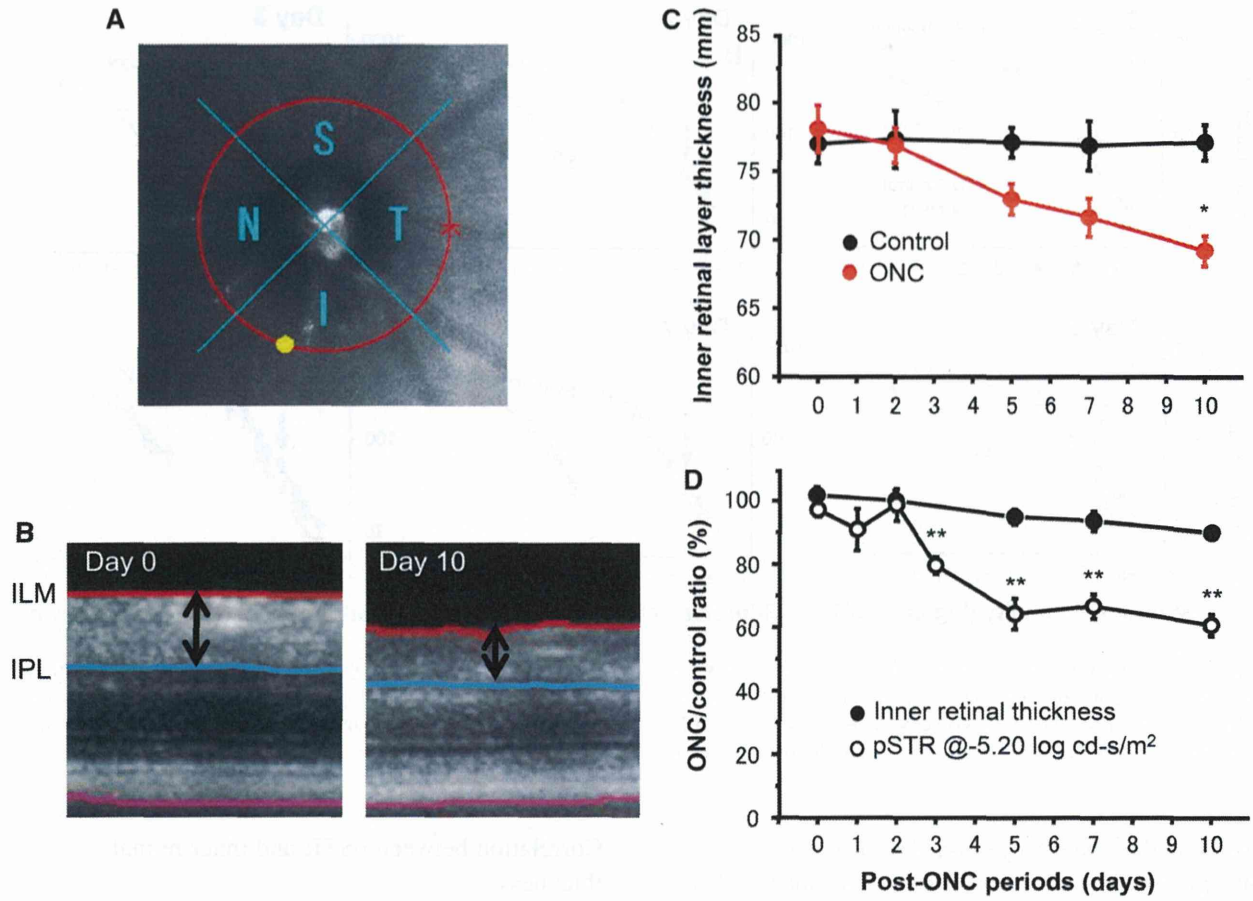

Fig. 4 SD-OCT images were acquired circumferentially around the optic nerve head (**a**). Representative SD-OCT images obtained from the same eye before (day 0, *left*) and after ONC (day 10, *right*) (**b**). The distance between the internal limiting membrane and inner plexiform layer was measured in order to determine the inner retinal thickness (indicated by the *arrow* in **b**). The inner retinal thickness was plotted against the post-ONC time course for the control and ONC eyes (**c**, $I = 9$ for each time point). The pSTR amplitude and inner retinal thickness of the ONC eyes were normalized to those of the contralateral control eyes, expressed as a percentage and plotted as a function of the post-ONC time course (**d**). *SD-OCT* spectral-domain optical coherence tomography, *ONC* optic nerve crush, *S* superior, *T* temporal, *I* inferior, *N* nasal, *ILM* internal limiting membrane, *IPL* inner plexiform layer, *pSTR* positive scotopic threshold response, *error bars* standard error, $^*P < 0.01$

patients with traumatic optic neuropathy, the PhNR, which reflects RGC function, deteriorates before there is significant loss of retinal nerve fiber layer thickness [10]. Taken together, these findings therefore suggest that functional alterations in the RGCs precede the anatomical loss of the RGCs themselves.

We also observed the expression of genes that determine specific RGC types [24, 25] as early as day 1. This molecular alteration preceded the functional and morphological changes detected by the pSTR or SD-OCT, indicating that changes at the molecular level have begun, while RGCs are still preserved and functioning.

A recent study of the changes induced by ONC found that pSTR began to decrease on day 7 [26], in contrast to our finding that a reduction had already occurred on day 3. This discrepancy may be due to a number of possible factors. First, we performed ONC by crushing the optic nerve with forceps for 5 s, while Lui et al. crushed the optic nerve for only 4 s. This difference could explain the earlier manifestation of the loss of RGC function in our study. Second, we normalized the pSTR amplitude to the value of the contralateral untreated eye, in order to reduce the influence of inter-animal variation and improve the sensitivity of our experiment. Therefore, we believe

that the sensitivity of our measurements was relatively high, lending credence to our findings.

One of the previously noted limitations of measuring RGC function with the ERG is that RGC function depends on inputs from upstream neurons such as photoreceptors and bipolar cells [16]. However, we found that the a- and b-waves, which depend on the function of the photoreceptors and bipolar cells, remained unchanged after ONC throughout the experiment, indicating that ONC did not affect the function of these upstream neurons. This suggests that alterations in the pSTR reflect abnormal function of the RGCs.

RGC function can also be evaluated by measuring pattern ERG in mice [27]. However, it has not been determined how early after ONC, the pattern ERG begins to deteriorate in mice. Measuring the visual evoked potential (VEP) is another method of evaluating RGC function. However, ONC immediately suppresses the VEP, even while RGCs continue to survive for some time. Therefore, measurements of the VEP cannot serve as markers of RGC function in experiments using ONC. In conclusion, we confirmed that changes in the pSTR reflected early losses of RGC function after ONC, raising the possibility that the pSTR could be used in monitoring the effects of novel therapies to protect RGCs in the early stages of degeneration. Furthermore, changes in RGC-specific gene expression preceded anatomical and functional changes in the RGCs themselves.

Acknowledgments We thank Ms. Junko Sato for her technical assistance. This work was supported in part by JSPS KAKENHI Grants-in-Aid for Scientific Research B (T.N. 26293372) and for Challenging Exploratory Research (Y.T. 26670263 and T.N. 26670751). This study was also supported by the JST Center for Revitalization Promotion (Y.T. and T.N.).

Conflict of interest The authors have no conflict of interest.

References

1. Heijl A, Leske MC, Bengtsson B, Hyman L, Bengtsson B, Hussein M, Early Manifest Glaucoma Trial G (2002) Reduction of intraocular pressure and glaucoma progression: results from the Early Manifest Glaucoma Trial. Arch Ophthalmol 120(10):1268–1279
2. Collaborative Normal-Tension Glaucoma Study Group (1998) The effectiveness of intraocular pressure reduction in the treatment of normal-tension glaucoma. Am J Ophthalmol 126(4):498–505
3. Musch DC, Gillespie BW, Lichter PR, Niziol LM, Janz NK, Investigators CS (2009) Visual field progression in the Collaborative Initial Glaucoma Treatment Study the impact of treatment and other baseline factors. Ophthalmology 116(2):200–207. doi:10.1016/j.ophtha.2008.08.051
4. Ryu M, Yasuda M, Shi D, Shanab AY, Watanabe R, Himori N, Omodaka K, Yokoyama Y, Takano J, Saido T, Nakazawa T (2012) Critical role of calpain in axonal damage-induced retinal ganglion cell death. J Neurosci Res 90(4):802–815. doi:10.1002/jnr.22800
5. Himori N, Yamamoto K, Maruyama K, Ryu M, Taguchi K, Yamamoto M, Nakazawa T (2013) Critical role of Nrf2 in oxidative stress-induced retinal ganglion cell death. J Neurochem 127(5):669–680. doi:10.1111/jnc.12325
6. Fujita Y, Sato A, Yamashita T (2013) Brimonidine promotes axon growth after optic nerve injury through Erk phosphorylation. Cell Death Dis 4:e763. doi:10.1038/cddis.2013.298
7. Yasuda M, Tanaka Y, Ryu M, Tsuda S, Nakazawa T (2014) RNA sequence reveals mouse retinal transcriptome changes early after axonal injury. PLoS One 9(3):e93258. doi:10.1371/journal.pone.0093258
8. Viswanathan S, Frishman LJ, Robson JG, Harwerth RS, Smith EL 3rd (1999) The photopic negative response of the macaque electroretinogram: reduction by experimental glaucoma. Invest Ophthalmol Vis Sci 40(6):1124–1136
9. Viswanathan S, Frishman LJ, Robson JG, Walters JW (2001) The photopic negative response of the flash electroretinogram in primary open angle glaucoma. Invest Ophthalmol Vis Sci 42(2):514–522
10. Gotoh Y, Machida S, Tazawa Y (2004) Selective loss of the photopic negative response in patients with optic nerve atrophy. Arch Ophthalmol 122(3):341–346. doi:10.1001/archopht.122.3.341
11. Rangaswamy NV, Frishman LJ, Dorotheo EU, Schiffman JS, Bahrani HM, Tang RA (2004) Photopic ERGs in patients with optic neuropathies: comparison with primate ERGs after pharmacologic blockade of inner retina. Invest Ophthalmol Vis Sci 45(10):3827–3837. doi:10.1167/iovs.04-0458
12. Miyata K, Nakamura M, Kondo M, Lin J, Ueno S, Miyake Y, Terasaki H (2007) Reduction of oscillatory potentials and photopic negative response in patients with autosomal dominant optic atrophy with OPA1 mutations. Invest Ophthalmol Vis Sci 48(2):820–824. doi:10.1167/iovs.06-0845
13. Machida S, Gotoh Y, Toba Y, Ohtaki A, Kaneko M, Kurosaka D (2008) Correlation between photopic negative response and retinal nerve fiber layer thickness and optic disc topography in glaucomatous eyes. Invest Ophthalmol Vis Sci 49(5):2201–2207. doi:10.1167/iovs.07-0887
14. Wang J, Cheng H, Hu YS, Tang RA, Frishman LJ (2012) The photopic negative response of the flash electroretinogram in multiple sclerosis. Invest Ophthalmol Vis Sci 53(3):1315–1323. doi:10.1167/iovs.11-8461
15. Machida S, Raz-Prag D, Fariss RN, Sieving PA, Bush RA (2008) Photopic ERG negative response from amacrine cell signaling in RCS rat retinal degeneration. Invest Ophthalmol Vis Sci 49(1):442–452. doi:10.1167/iovs.07-0291
16. Bui BV, Fortune B (2004) Ganglion cell contributions to the rat full-field electroretinogram. J Physiol 555(Pt 1):153–173. doi:10.1113/jphysiol.2003.052738

17. Sieving PA, Frishman LJ, Steinberg RH (1986) Scotopic threshold response of proximal retina in cat. J Neurophysiol 56(4):1049–1061
18. Frishman LJ, Shen FF, Du L, Robson JG, Harwerth RS, Smith EL 3rd, Carter-Dawson L, Crawford ML (1996) The scotopic electroretinogram of macaque after retinal ganglion cell loss from experimental glaucoma. Invest Ophthalmol Vis Sci 37(1):125–141
19. Mojumder DK, Sherry DM, Frishman LJ (2008) Contribution of voltage-gated sodium channels to the b-wave of the mammalian flash electroretinogram. J physiol 586(10):2551–2580. doi:10.1113/jphysiol.2008.150755
20. Smith BJ, Wang X, Chauhan BC, Cote PD, Tremblay F (2014) Contribution of retinal ganglion cells to the mouse electroretinogram. Doc Ophthalmol Adv Ophthalmol. doi:10.1007/s10633-014-9433-2
21. Shanab AY, Nakazawa T, Ryu M, Tanaka Y, Himori N, Taguchi K, Yasuda M, Watanabe R, Takano J, Saido T, Minegishi N, Miyata T, Abe T, Yamamoto M (2012) Metabolic stress response implicated in diabetic retinopathy: the role of calpain, and the therapeutic impact of calpain inhibitor. Neurobiol Dis 48(3):556–567. doi:10.1016/j.nbd.2012.07.025
22. Alarcon-Martinez L, Aviles-Trigueros M, Galindo-Romero C, Valiente-Soriano J, Agudo-Barriuso M, Villa Pde L, Villegas-Perez MP, Vidal-Sanz M (2010) ERG changes in albino and pigmented mice after optic nerve transection. Vision Res 50(21):2176–2187. doi:10.1016/j.visres.2010.08.014
23. Kohzaki K, Vingrys AJ, Bui BV (2008) Early inner retinal dysfunction in streptozotocin-induced diabetic rats. Invest Ophthalmol Vis Sci 49(8):3595–3604. doi:10.1167/iovs.08-1679
24. Shi M, Kumar SR, Motajo O, Kretschmer F, Mu X, Badea TC (2013) Genetic interactions between Brn3 transcription factors in retinal ganglion cell type specification. PLoS One 8(10):e76347. doi:10.1371/journal.pone.0076347
25. Sajgo S, Ghinia MG, Shi M, Liu P, Dong L, Parmhans N, Popescu O, Badea TC (2014) Dre-cre sequential recombination provides new tools for retinal ganglion cell labeling and manipulation in mice. PLoS One 9(3):e91435. doi:10.1371/journal.pone.0091435
26. Liu Y, McDowell CM, Zhang Z, Tebow HE, Wordinger RJ, Clark AF (2014) Monitoring retinal morphologic and functional changes in mice following optic nerve crush. Invest Ophthalmol Vis Sci 55(6):3766–3774. doi:10.1167/iovs.14-13895
27. Porciatti V (2007) The mouse pattern electroretinogram. Doc Ophthalmol Adv Ophthalmol 115(3):145–153. doi:10.1007/s10633-007-9059-8

nata (as required), which did not affect the risk of having a case of post-intravitreal injection endophthalmitis ($P = 0.503$). In the multivariate analysis, no potentially modifiable risk factors were identified to increase post-intravitreal injection endophthalmitis.

This survey sought to establish some of the practices of Victorian ophthalmologists who perform intravitreal injections to treat neovascular AMD, mainly in their private rooms. Although no potentially modifiable risk factors are identified for post-intravitreal injection endophthalmitis, some trends are shown. Of particular interest are the trends for those who see more patients and those who do not use a drape, and while these two factors are not linked, it is not possible to hypothesize whether 'time' is a factor. Major limitations of this study include the potential low number of responses, volunteer bias with an under-participation of those who may have had endophthalmitis and the retrospective design.

The authors are pleased to report that current practices in Victoria are consistent with current evidence. We thank all those who participated and believe that the information from this survey explores and helps ophthalmologists to keep thinking about potentially modifiable risk factors for optimal management in the prevention of post-intravitreal injection endophthalmitis.

Danielle A Buck MBBS BSc,[1]
Rosie Dawkins MBBS MPH,[1]
Ryo Kawasaki MD PhD,[2,3]
Sukhpal S Sandhu MD FRANZCO[1,3,4]
and Penelope J Allen FRANZCO[1,3,4]
[1]Royal Victorian Eye and Ear Hospital, [3]Centre for Eye Research Australia, and [4]University of Melbourne, Melbourne, Victoria, Australia; and [2]Yamagata University Faculty of Medicine, Yamagata, Japan
Received 15 March 2014; accepted 30 July 2014.

References

1. Harvey KJ, Day RO, Campbell WG *et al.* Saving money on the PBS: ranibizumab or bevacizumab for neovascular macular degeneration? *Med J Aust* 2011; **194**: 567–8.
2. Chen E, Lin MY, Cox J *et al.* Endophthalmitis after intravitreal injection: the importance of viridans streptococci. *Retina* 2011; **31**: 1525–33.
3. Lyall DA, Tey A, Foot B *et al.* Post-intravitreal anti-VEGF endophthalmitis in the United Kingdom: incidence, features, risk factors, and outcomes. *Eye* 2012; **26**: 1517–26.
4. McCannel CA. Meta-analysis of endophthalmitis after intravitreal injection of anti-vascular endothelial growth factor agents: causative organisms and possible prevention strategies. *Retina* 2011; **31**: 654–61.
5. Shah CP, Garg SJ, Vander JF *et al.* Outcomes and risk factors associated with endophthalmitis after intravitreal injection of anti-vascular endothelial growth factor agents. *Ophthalmology* 2011; **118**: 2028–34.

Regional correlation of macular areas and visual acuity in patients with open-angle glaucoma

Good vision is closely associated with quality of life (QOL). Visual function in eyes with retinal disease has two important parameters: the visual field (VF) and visual acuity (VA). Generally, QOL-affecting VF loss is a common symptom in glaucoma patients, and can lead to driving license revocation and reduced reading speed.[1] QOL can also be significantly disturbed by decreased VA. Recent studies have revealed that macular lesions are common in open-angle glaucoma (OAG).[2] However, there is currently only a limited understanding of the regional correlation of VA in the macular function. A greater understanding of these regional correlations would help diagnose the cause of decreased VA in patients and therefore be of significant clinical value. The purpose of this investigation was thus to determine the regional correlation of VA to sensitivity in the test points of the Humphrey field analyser 10-2 programme (HFA 10-2) or to optical coherence tomography (OCT) macular maps in patients with OAG.

This study included 60 eyes with OAG. The inclusion criteria were: OAG with a glaucomatous VF according to the Anderson-Patella classification and spherical equivalent (SE) refractive error of ≥8.00 D (i.e. excluding high myopia). The exclusion criteria were: decimal VA <0.3 and the presence of VF-affecting ocular or systemic diseases other than OAG. Best-corrected VA was measured with a standard Japanese decimal VA chart and converted to the logarithm of the minimum angle of resolution (logMAR) for statistical analysis. To assess macular function, HFA 10-2 threshold values, total deviation (TD) and pattern deviation (PD) were examined in reliably measured VFs (excluding measurements with <20% fixation errors and <33% false-positive or false-negative results). OCT (3D OCT-2000; TOPCON Corporation, Topcon Corporation, Tokyo, Japan) was used to measure the retinal nerve fibre layer (RNFL), ganglion cell complex (GCC) and ganglion cell layer plus inner plexiform layer (GCL + IPL) of the maps based on macular cube scans of a 6 × 6 mm square area centered on the fovea. Scans with image quality less than 70 or with inaccurate segmentation were excluded. All the examinations were performed within 3 months. Spearman's rank correlation coefficient was used to analyse the correlation between logMAR and each of the 68 HFA 10-2 test points, as well as the

Competing/conflicts of interest: No stated conflict of interest.

Funding sources: This paper was supported in part by a JST grant from JSPS KAKENHI Grants-in-Aid for Scientific Research (B) (T.N. 26293372) and for Exploratory Research (T.N. 26670751), and by JST Center for Revitalization Promotion.

This retrospective study was approved by the institutional review board of Tohoku University Graduate School of Medicine (study 2012-1-574).

This paper was presented at the Association of Research Visual Science 2013.

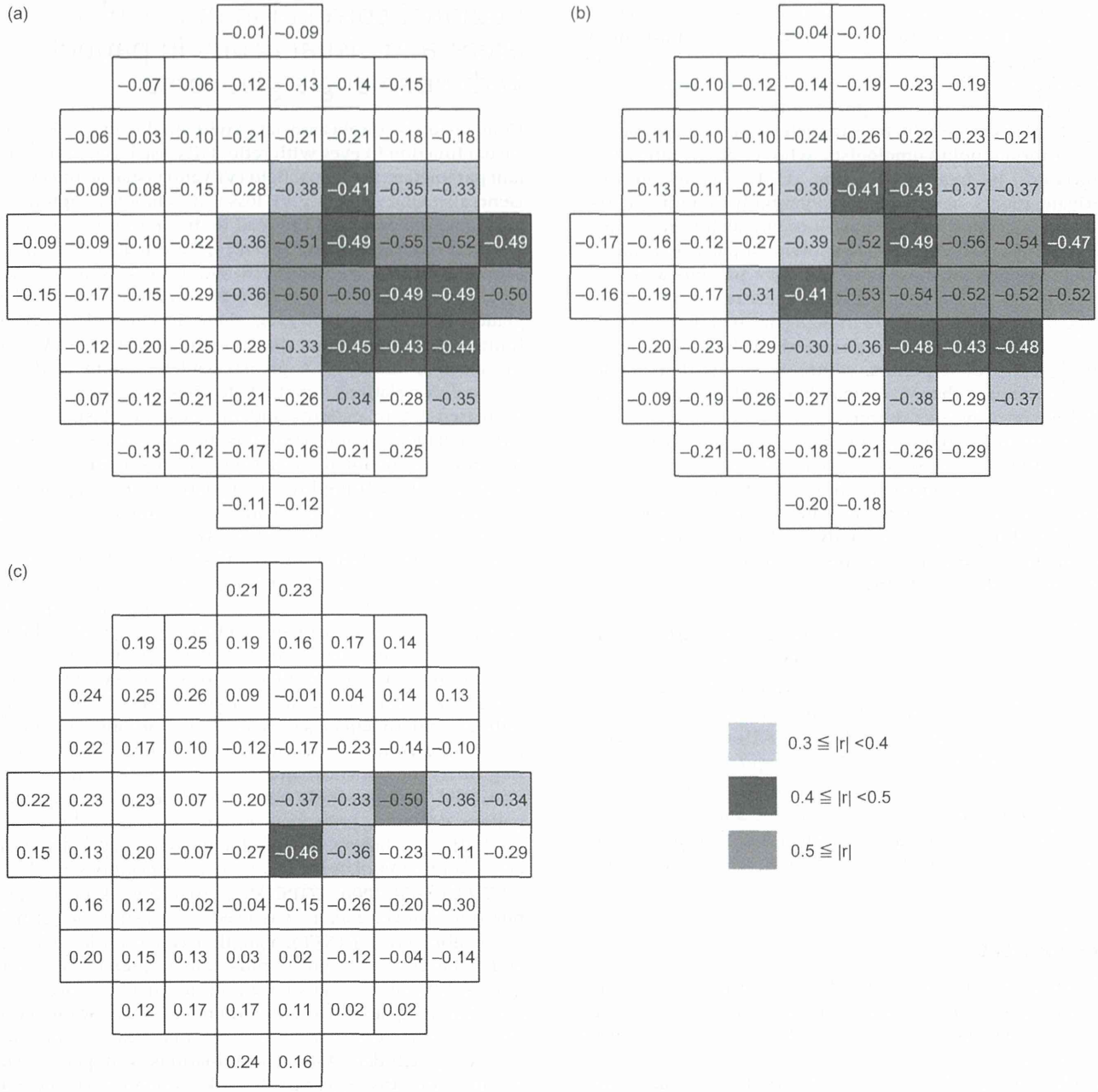

Figure 1. Distribution of Humphrey field analyser 10-2 programme (HFA 10-2) tests points correlated with visual acuity (VA). The grey-scale maps show the correlation coefficient of VA and HFA 10-2 measurements of threshold (a), total deviation (b) and pattern deviation (c). The right side of the figure represents the temporal visual field (the disc side) and the left side represents the nasal visual field. Darker shades of grey indicate a higher correlation coefficient, with a step scale of 0.1. Test points shown in white had no statistically significant correlation.

correlation between logMAR and each point on a 10×10 grid overlaid on the OCT macular maps.

Average demographic data for the patients in this study were as follows: age was 65.7 ± 11.1 years, SE was -2.8 ± 2.2 D, logMAR was 0.08 ± 0.28, HFA 30-2 mean deviation was -12.1 ± 8.9 dB, baseline intraocular pressure was 13.0 ± 3.2 mmHg and circumpapillary retinal nerve fibre layer thickness (cpRNFLT) was 79.3 ± 14.8 μm. Figure 1 shows the distribution of significantly VA-correlated HFA 10-2 test points. Test points with significantly VA-correlated threshold values (r = −0.36 to −0.55), TD (r = −0.39 to −0.56) and PD (r = −0.33 to −0.50) were mainly located in the area of the papillomacular bundle (PMB). Figure 2 shows the distribution of significantly VA-correlated grid points in the OCT macular maps. In the RNFL and GCC maps, the correlation coefficient with VA ranged from −0.30 to −0.54 and from −0.30 to −0.50, respectively. In these maps, the areas of significantly